NASA TECHNICAL NOTE

NASA TN D-4452

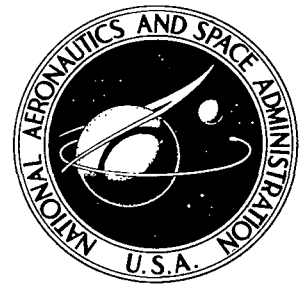

RADIATION DAMAGE IN THICK COPPER AND GOLD SPECIMENS PRODUCED BY LOW-ENERGY PROTONS

by Howard F. Savage and Robert D. Morris

Ames Research Center
Moffett Field, Calif.

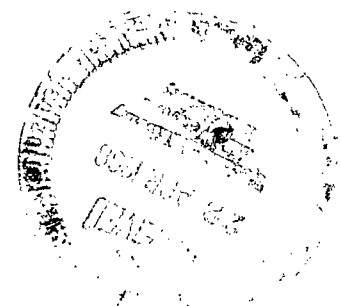

NATIONAL AERONAUTICS AND SPACE ADMINISTRATION • WASHINGTON, D. C. • APRIL 1968

RADIATION DAMAGE IN THICK COPPER AND GOLD SPECIMENS PRODUCED BY LOW-ENERGY PROTONS

By Howard F. Savage and Robert D. Morris

Ames Research Center
Moffett Field, Calif.

NATIONAL AERONAUTICS AND SPACE ADMINISTRATION

For sale by the Clearinghouse for Federal Scientific and Technical Information
Springfield, Virginia 22151 – CFSTI price $3.00

RADIATION DAMAGE IN THICK COPPER AND GOLD SPECIMENS PRODUCED BY LOW-ENERGY PROTONS

By Howard F. Savage and Robert D. Morris

Ames Research Center

SUMMARY

The production of defects at 90° K in thick gold and copper foils by 50 to 400 keV protons and subsequent annealing characteristics of these metals have been studied. The thickness of the specimens was several times the calculated range of the protons. The defects formed in gold were uniformly distributed along the proton range, whereas the defects formed in copper were more than twice as dense toward the end of the range as at the beginning. At doses from 10^{15} protons/cm^2 to at least the maximum of the tests, the change in electrical resistivity of both the gold and copper at incident energies between 50 and 400 keV can be described by a relation of the form $\Delta\rho = A\varphi^n$, where $\Delta\rho$ is the increase in resistivity and φ is the dose. The recovery of gold upon isochronal annealing was similar to that observed for high-energy irradiations of thin specimens.

INTRODUCTION

This work was undertaken to investigate the defects produced in thick foils of gold and copper by low-energy protons and the behavior of these defects during subsequent annealing. Specimens several times thicker than the mean range of the protons were chosen because, for actual radiation damage problems in space, all except the very energetic particles come to rest within the space vehicle components. The defects consist of atoms displaced from their normal lattice positions along with the resulting vacancies. This damage causes measurable changes in the material properties such as length, volume, hardness, yield stress, and electrical resistivity. The changes in electrical resistivity were used in this experiment as the measure of damage caused by the proton irradiations.

Several high-energy (greater than 10 MeV) proton irradiation experiments (refs. 1-3) have been performed on gold and copper. In these the protons were sufficiently energetic to pass through the samples with but a small energy loss, and thus produced a defect concentration quite homogeneous throughout the thickness of the sample. The previously reported low-energy-proton irradiation experiments have shown differing results. When Anspaugh (ref. 4) bombarded thick copper foils with protons and helium ions, which were stopped in the specimen, he found that the number of defects was much less than predicted by theoretical calculations, the difference being much more pronounced at 50 than at 300 keV. On the other hand, when Schmidtke (ref. 5) bombarded very thin (1.3×10^{-5} cm) gold foils through which even his lowest energy protons

(80 keV) passed without large energy losses, he found that the number of defects differed from that predicted by only a constant factor over the proton energy range from 80 to 1.4 MeV.

In the present experiment, where the proton range was less than the sample thickness, the energy at which the defects were produced varied from the incident energy downward to the threshold displacement energy. The concentration of defects through the thickness of the specimen was expected to be inhomogeneous since the number of displacements produced should vary with the proton energy. In addition, the incident protons would probably be trapped in the sample as a defect. The purpose of the present study was to determine how the damage varied at low energies and to indicate, by annealing studies, whether or not the defects formed along the range of the protons had the same configuration at high and low incident proton energies. Copper and gold were selected for the irradiations since thin specimens of these had been studied extensively at higher proton energies and the defect production in copper could be compared with similar low-energy, thick-film results by Anspaugh (ref. 4).

EXPERIMENTAL PROCEDURE

The change in electrical resistivity of the irradiated specimens was determined from a comparison of the potential difference at 90° K across the irradiated specimen with that across a similar specimen that was shielded from the irradiation. A current of about 75 mA was passed in series through the irradiated and the shielded specimens. A series of separate readings of the potential difference across the irradiated and shielded specimens was taken with a 5-digit digital voltmeter having a least count of 0.1 μV. The ratio of these potential differences was also the resistivity ratio. In the calculation of the percent increase in the resistivity of the damaged region of the irradiated specimen, the specimen was considered to be two resistances in parallel, one with a thickness equal to the calculated mean proton range (ref. 6) and the other with the thickness of the remaining part of the specimen. The calculated ranges of a 400 keV proton in gold and copper, respectively, are 2.08×10^{-4} cm and 2.24×10^{-4} cm.

The isochronal annealing data were obtained by holding the specimens for 30 min at temperatures successively 10° K higher than the previous anneal. The change in resistivity at 90° K was measured after each anneal.

In the sections below, the proton accelerator, specimen mounting, temperature control, and the errors in the experiment will be discussed.

Accelerator

A Van de Graaff accelerator, equipped with a beam analyzing magnet and an electrostatic beam scanner, accelerated hydrogen ions to the desired energy in the range between 50 and 400 keV; then they were focused through the analyzing magnet which was set to deflect the proton beam into the electrostatic scanner

which, in turn, uniformly scanned the beam over a 10 by 10 cm area at the specimen location. All but a 1.3 by 3.8 cm rectangle from the center of the 100 cm^2 scanned beam was intercepted by the liquid-nitrogen-cooled shroud surrounding the specimens. The current density was measured by monitoring the charge intercepted by a disk (with a 29 cm^2 area) which contained the rectangular aperture.

The vacuum system was pumped by two oil diffusion pumps equipped with cryogenically cooled baffles. The base pressure of the system was 4×10^{-7} torr with the proton beam on.

Specimen Preparation and Mounting

Figure 1 is a schematic drawing of a set of specimens mounted on the holder. The holder was made from 0.032-inch-thick copper strips 0.25 inch wide and was attached to a liquid-nitrogen reservoir by a 2-inch-long, 0.08-

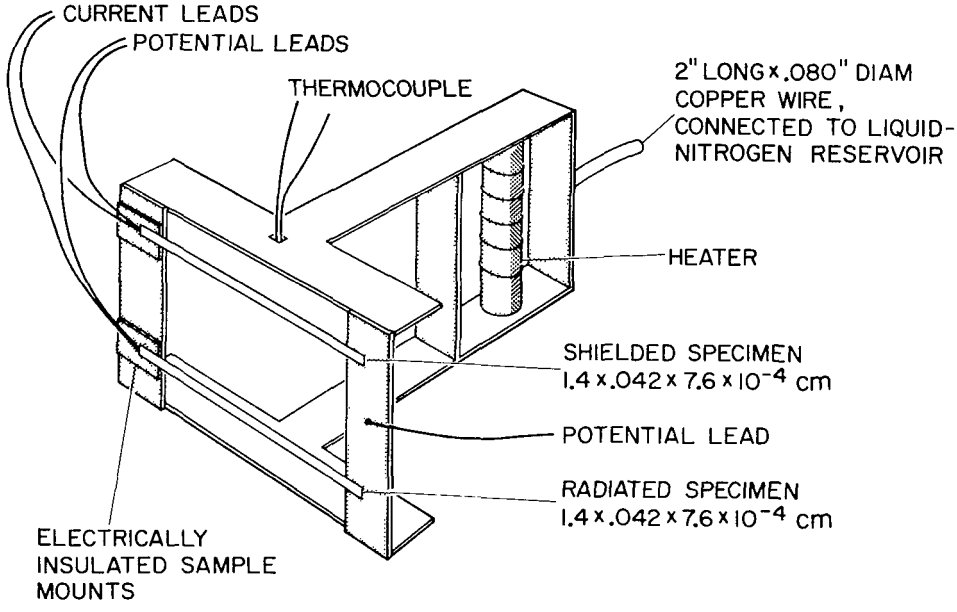

Figure 1.- Schematic drawing of the specimen holder.

inch-diameter copper wire to provide a high-conductance thermal path. When mounted in the vacuum test chamber, the holder and reservoir were inside a liquid-nitrogen-cooled shroud. The only opening between the vacuum chamber and the specimens was the rectangular aperture for admitting the proton beam. The geometry of the specimen holder was chosen to minimize temperature gradients and to permit quick temperature changes. The specimen temperature could be raised 2° K per second with the 10-W heater. The electrically insulated mounts for the specimen were made with 0.5-mil mylar sheet, bonded with silicon varnish, between thin copper strips.

The gold and copper ribbons were obtained commercially and had stated purities of 99.999 percent. Single specimens of gold and copper were used throughout the tests. Each was pressed in a mandrel to reduce its thickness

from 10^{-3} to 7.6×10^{-4} cm. The average reduced thickness was determined from the measured surface areas and masses and the handbook values of the densities. The samples were nominally 1.4 cm long by 0.042 cm wide. The gold specimens were cleaned consecutively with acetone, methanol, boiling distilled water, NHO_3, and HCl. Then they were annealed for 2 hours at 575° K in air and soldered to the specimen holder. The test chamber was then evacuated and the specimens were annealed at 400° K for 24 hours. The copper specimens were cleaned consecutively with HNO_3, HCl, and distilled water. They were then soldered to the specimen holder and annealed at 400° K for 72 hours in a vacuum.

Temperature Control

The specimen temperature was measured with a Au-2.1 percent Co vs. Ag-0.37 percent Au thermocouple soldered to the specimen holder (fig. 1). The temperature was controlled by sensing the difference between the thermocouple electromotive force and a voltage supplied by a precision microvolt source preset to the point that represented the desired temperature. When the specimen temperature exceeded the set temperature, the heater power was automatically reduced by about 2 percent until the temperature fell below the set-point, at which time full set-point power was restored. At the beginning of a temperature change, the heater power was controlled manually until the set temperature was reached. The temperature was controlled to ±0.1° K at temperatures below about 250° K and to ±0.2° K above 250° K.

Errors

Both systematic and random error sources were considered. The systematic errors, due to uncertainty in the specimen thickness and in the proton range, are estimated to cause errors in the change in resistivity no greater than approximately ±5 percent of the change at 58 keV and ±1.5 percent at 400 keV for doses greater than 10^{14} protons/cm^2. The random fluctuations in the proton energy were of the order of ±5 keV at all energies. The estimated error in the measurement of the dose is about ±5 percent. Random errors in measuring the change in resistivity were determined by measuring the resistance at the same point a number of times. The probable error of the resistance readings taken for a data point is of the order of ±0.02 percent.

RESULTS AND DISCUSSION

The resistivity changes for gold and copper will be discussed first as a function of dose at constant energy, and then as a function of energy at a constant dose. Finally, the isochronal annealing of gold and copper will be discussed and compared with results obtained by others.

Damage as a Function of Dose

The increase in resistivity of the damaged region of the gold and copper specimens as a function of dose, as shown in figure 2 for a proton energy of 204 keV, is similar at all energies between 58 and 404 keV. That is, for

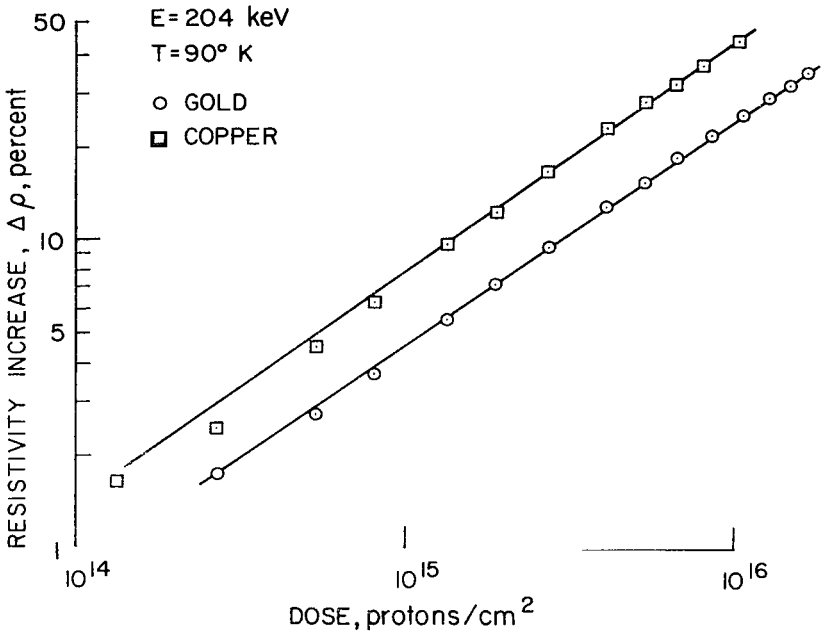

Figure 2.- Production of damage at 90° K in gold and copper by 204 keV protons.

doses between about 10^{15} protons/cm^2 and the maximum of the tests, each could be approximated with a straight line when the logarithm of $\Delta\rho$, the increase in resistivity, was plotted against the logarithm of φ, the dose. Thus, the data at these doses can be represented by a power law relation of the form $\Delta\rho = A\varphi^n$, where A and n are constants for a particular proton energy. The values of A and n for each incident proton energy used are listed in table I. The three values at 404 keV for gold represent three separate sets of data and are a measure of the repeatability of the data and of variations in experimental conditions. As indicated above, there are deviations from straight lines exceeding experimental error (e.g., the copper data of fig. 2) at doses below about 10^{15} protons/cm^2. This is to be expected since, at very low doses, traps should far outnumber radiation induced defects and the increase in resistivity should then be directly proportional to dose, that is, n = 1.

Walker (ref. 7) has shown that both the production and recovery of electron-induced damage in copper at liquid-nitrogen temperatures were dominated by the interaction of induced defects with other crystal imperfections. In Walker's model, the interstitials go to trapping sites without interacting with each other. He assumed that the resistivity of a given concentration of interstitials was constant whether or not they were trapped. If only unsaturable traps (dislocations, for example) were present, then $\Delta\rho = A\varphi^{0.5}$ at high doses. If only nucleation traps (that is, traps in which the capture of an interstitial enhances the probability of subsequent capture of interstitials

at that site) were present, then $\Delta\rho = A\varphi$ at high doses. If traps far outnumbered radiation-induced defects, then $\Delta\rho = A\varphi$ for all doses.

The data tabulated in table I and represented by figure 2, for both gold and copper, have values of the exponent between 0.6 and 0.9. Thus, if proton damage is similar to electron damage, the interstitial trapping sites probably would consist of a mixture of unsaturable and nucleation traps. Also, it is indicated that the total number of traps does not greatly exceed the number of defects produced (otherwise, n = 1 as noted above).

Damage as a Function of Energy

In figure 3, the increases in resistivity as a function of initial proton energy are presented for a dose of 5×10^{15} protons/cm^2. Results for other

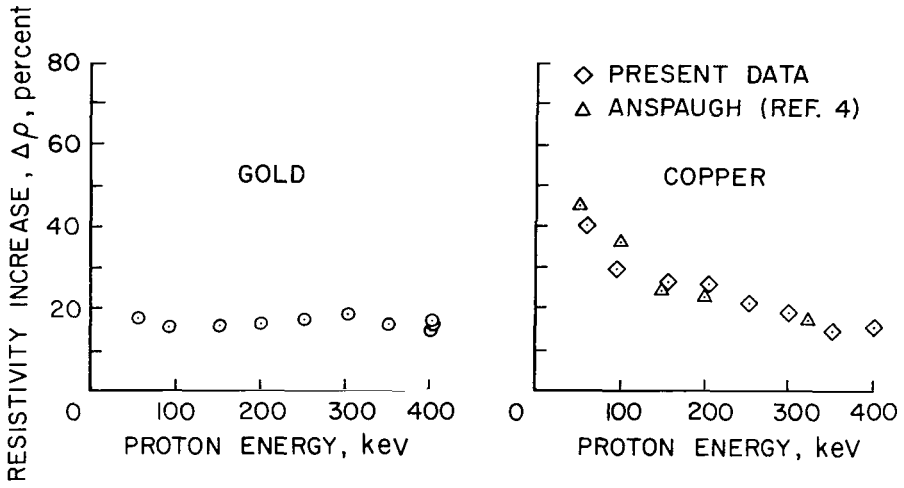

Figure 3.- Increase in resistivity of gold and copper at 90° K as a function of initial proton energy.

doses are similar. The copper data of Anspaugh (ref. 4), adjusted to agree with the present results at 400 keV, are also shown for comparison.

The damage was essentially constant at all energies for the gold specimen, as indicated by the nearly constant increase in resistivity for protons with initial energy between 50 and 400 keV. Thus, the defects are apparently almost uniformly distributed along the range of the incident protons. For the copper specimen, the resistivity showed about a twofold increase when the incident proton energy was decreased from 400 to 50 keV.

The number of atoms displaced by an energetic proton as it is brought to rest inside a gold or copper specimen can be calculated from theory (ref. 4) in combination with experimental stopping-power data. These calculations indicate that, in being brought to rest, a proton with 50 keV initial energy should displace about half as many gold atoms as a proton with 400 keV initial energy. On the other hand, the range of a 400-keV proton is about five times the range of a 50-keV proton in gold. Thus, in a gold specimen, the average number density of vacancy-interstitial pairs along the path of a 50-keV proton should be roughly 4 times that along the path of a 400-keV proton as it is slowed from 400 to 50 keV; correspondingly, the increase in resistivity averaged over the range of a 50-keV proton should be 4 times greater than that averaged over the range of a 400-keV proton in slowing down to 50 keV. For a

copper specimen, the calculations show that a 50-keV proton should displace about two-thirds as many copper atoms as a 400-keV proton; thus, the average number density of vacancy-interstitial pairs and thus, the increase in resistivity caused by a 50-keV proton should be even higher in copper in comparison to the 400-keV proton than in gold.

The trend of the present data shown in figure 3 for copper is consistent with the calculations mentioned above and the results agree well with those obtained by Anspaugh (ref. 4) for thick copper specimens. But the trend of the data for gold does not agree with either the above calculations or the results obtained by Schmidtke (ref. 5) for thin gold specimens. He found a resistivity change about three times greater at 50 keV than at 400 keV. However, for α particles in gold at 77° K, Stangler (ref. 8) found an opposite trend, that is, about four times as much damage in the first half of the range as in the second half.

Thus, a question arises when the present results for gold are compared with those for copper. Why does the defect concentration remain constant along the proton range in gold, but increase toward the end of the range in copper? The present copper data and that of Anspaugh (ref. 4) are in general agreement with each other and with the calculated trend. However, the gold data are very inconsistent in that results have been reported that agree (ref. 5) and disagree (ref. 8) with the calculated trend. Some unknown material parameters must be causing the disagreement since there is no other apparent reason for the results to differ from either the copper results or from the calculated trend. None of the obvious differences between copper and gold seem to provide a basis for explaining the observed difference.

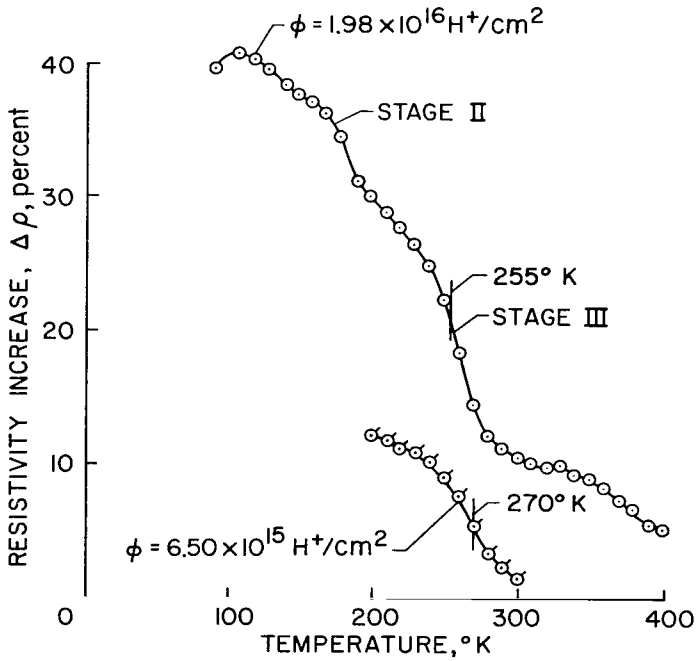

Figure 4.- Isochronal recovery of gold specimen irradiated with 404 keV protons at 90° K; time increment = 30 minutes.

Isochronal Annealing of Gold

The representative isochronal recovery curves shown in figure 4 were obtained by annealing the irradiated specimens for 30-minute periods at successive 10° K increments starting at 100° K. The change in resistivity at 90° K was measured after each anneal. The temperature increment was selected so that sufficient data would be obtained to define the recovery stages; the annealing time increment was chosen so that there would be appreciable annealing with each increase in temperature during the recovery stages. Similar data were obtained for copper, but are not presented

since the recovery was very complex and no analysis could be done to determine the factors involved in the recovery.

The annealing characteristics for gold after a dose of 2×10^{16} H^+/cm^2 at 404 keV show a small recovery (stage II) at about 180° K and a large recovery (stage III) at about 255° K; these are the same as the characteristics reported by Dworschak and Koehler (ref. 2) for thin specimens and 10-MeV protons; it is, thus, indicated that the defect configurations are similar. The analysis of Bauer and Sosin (ref. 9) showed that, for second-order kinetics of the recovery process, a temperature shift of the annealing stage to a higher temperature would be expected if the concentration of defects in the specimen were decreased. No shift in temperature would be expected for first-order kinetics. Experimentally, a shift of the annealing stage (stage III) to a higher temperature, about 270° K, was observed for an irradiation to one-third the previous dose as shown in figure 4. Therefore, the stage III recovery process apparently obeys second-order kinetics. With this result, the analysis of Grenning and Koehler (ref. 3) was used to determine that the activation energy of the stage III recovery in the gold specimen was 0.89 ±0.05 eV. This value compares favorably with the 0.82 ±0.05 eV migration energy (ref. 10) of a single vacancy, indicating that vacancy migration may be responsible for the stage III recovery, as suggested by Dworschak and Koehler (ref. 2) for high-energy irradiations. Thus, the recovery of a thick gold specimen after irradiation by 404 keV protons is very similar to that found after high-energy, 10 MeV irradiations. This implies that the defects produced along the entire path of the 404 keV proton are nearly similar in configuration to those resulting from the high energy proton. If they were not, the activation energy (stage III) for their recovery would be different.

CONCLUDING REMARKS

The following remarks can be made as a result of irradiating thick gold and copper specimens at 90° K with protons in the 50 to 400 keV energy range:

1. The defects remaining in the gold specimen after irradiation were almost uniformly distributed along the range of the incident protons.

2. The average defect density of the copper specimen irradiated with 50-keV protons was more than twice that which resulted from a 400-keV irradiation.

3. Above about 10^{15} protons/cm^2 and at the test energies (50 to 400 keV), the change in electrical resistivity of both gold and copper as a function of dose could be described by a power law relationship between dose and energy.

4. For isochronal annealing, the recovery of the gold was not markedly different from that found by others after high-energy irradiations of thin specimens, indicating that the defect configurations are similar.

Ames Research Center
National Aeronautics and Space Administration
Moffett Field, Calif., 94035, Dec. 1, 1967
129-03-15-03-00-21

REFERENCES

1. Dworschak, F.; Herschbach, K.; and Koehler, J. S.: Experiments on Stage III Annealing in the Noble Metals. Phys. Rev., vol. 133, no. 1A, Jan. 6, 1964, pp. A293-A303.

2. Dworschak, F.; and Koehler, J.: Stage III Annealing in Proton-Irradiated Noble Metals. Phys. Rev., vol. 140, no. 3A, Nov. 1, 1965, pp. A941-A-953.

3. Grenning, D. A.; and Koehler, J. S.: Resistivity Recovery of Dilute Alloys of Silver, Copper, and Gold, Proton-Irradiated at 80° K. Phys. Rev., vol. 144, no. 2, April 15, 1966, pp. 439-457.

4. Anspaugh, B. E.: The Energy Dependence of Radiation Damage Induced in Copper by Low Energy H^1 and He^4 Ions. Ph.D. Thesis, University of Nebraska, Dec. 1964.

5. Schmidtke, M.: Messung der Anderung des Elektrischen Widerstandes von Gold bei Bestrahlung mit Monoenergetischen Protonen Variobler Energie. Z. Physik, vol. 188, no. 2, Oct. 1965, pp. 165-166.

6. Whaling, W.: The Energy Loss of Charged Particles in Matter. Handbuch der Physik, S. Flügge, ed., Springer, Berlin, 1958, vol. 34, pp. 193-217.

7. Walker, R. M: Electron-Induced Radiation Damage in Pure Metals. Proceedings E. Fermi International School of Physics, D. S. Billington, ed., Academic Press, Inc., N. Y., 1962, pp. 594-629.

8. Stangler, F.: The Influence of Point Defects on the Electrical Properties of Aluminum, Copper, and Gold at Liquid Nitrogen Temperatures. Appl. Materials Res., vol. 5, no. 1, Jan. 1966, pp. 53-55.

9. Bauer, W.; and Sosin, A.: Point Defect Studies in Gold by Electron Irradiation at Low Temperatures. II. Resistivity Recovery Spectrum from 15 to 240°K. Phys. Rev., vol. 136, no. 1A, Oct. 5, 1964, pp. A255-A261.

10. Bauerle, J. E.; and Koehler, J. S.: Quenched-In Lattice Defects in Gold. Phys. Rev., vol. 107, no. 6, Sept. 15, 1957, pp. 1493-1498.

TABLE I.- VALUES OF n AND A TO FIT DATA FOR $\Delta\rho = A\varphi^n$

Energy, keV	Gold		Copper	
	n	A, $(cm^2/H^+)^n$	n	A, $(cm^2/H^+)^n$
58	0.59	1.1×10^{-8}	0.90	3.0×10^{-13}
96	.66	5.4×10^{-10}	.81	5.9×10^{-12}
154	.76	1.8×10^{-11}	.71	1.9×10^{-10}
204	.71	1.2×10^{-10}	.73	8.5×10^{-11}
254	.73	5.4×10^{-11}	.68	4.0×10^{-10}
302	.77	1.6×10^{-11}	.69	3.0×10^{-10}
354	.71	1.0×10^{-10}	.68	3.5×10^{-10}
404	.73	5.2×10^{-11}	.79	7.5×10^{-12}
404	.70	1.4×10^{-10}		
404	.82	2.0×10^{-12}		

"The aeronautical and space activities of the United States shall be conducted so as to contribute . . . to the expansion of human knowledge of phenomena in the atmosphere and space. The Administration shall provide for the widest practicable and appropriate dissemination of information concerning its activities and the results thereof."

—NATIONAL AERONAUTICS AND SPACE ACT OF 1958

NASA SCIENTIFIC AND TECHNICAL PUBLICATIONS

TECHNICAL REPORTS: Scientific and technical information considered important, complete, and a lasting contribution to existing knowledge.

TECHNICAL NOTES: Information less broad in scope but nevertheless of importance as a contribution to existing knowledge.

TECHNICAL MEMORANDUMS: Information receiving limited distribution because of preliminary data, security classification, or other reasons.

CONTRACTOR REPORTS: Scientific and technical information generated under a NASA contract or grant and considered an important contribution to existing knowledge.

TECHNICAL TRANSLATIONS: Information published in a foreign language considered to merit NASA distribution in English.

SPECIAL PUBLICATIONS: Information derived from or of value to NASA activities. Publications include conference proceedings, monographs, data compilations, handbooks, sourcebooks, and special bibliographies.

TECHNOLOGY UTILIZATION PUBLICATIONS: Information on technology used by NASA that may be of particular interest in commercial and other non-aerospace applications. Publications include Tech Briefs, Technology Utilization Reports and Notes, and Technology Surveys.

Details on the availability of these publications may be obtained from:

SCIENTIFIC AND TECHNICAL INFORMATION DIVISION

NATIONAL AERONAUTICS AND SPACE ADMINISTRATION

Washington, D.C. 20546